Na^+ and Ca^{2+} Effect on the Hydration and Orientation of the Phosphate Group of DPPC at Air−Water and Air−Hydrated Silica Interfaces

Nadia N. Casillas-Ituarte, Xiangke Chen, Hardy Castada, and Heather C. Allen*

Department of Chemistry, The Ohio State University, 100 West 18th Avenue, Columbus, Ohio 43210

Received: March 11, 2010; Revised Manuscript Received: June 14, 2010

Hydration and orientation of the phosphate group of dipalmitoylphosphatidylcholine (DPPC) monolayers in the liquid-expanded (LE) phase and the liquid-condensed (LC) phase in the presence of sodium ions and calcium ions was investigated with vibrational sum frequency generation (SFG) spectroscopy at the air-aqueous interface in conjunction with surface pressure measurements. In the LE phase, both sodium and calcium affect the phosphate group hydration. In the LC phase, however, sodium ions affect the phosphate hydration subtly, while calcium ions cause a marked dehydration. Silica-supported DPPC monolayers prepared by the Langmuir−Blodgett method reveal similar hydration behavior relative to that observed in the corresponding aqueous subphase for the case of water and in the presence of sodium ions. However, in the presence of calcium ions the phosphate group dehydration is greater than that from the corresponding purely aqueous $CaCl_2$ subphase. The average tilt angles from the surface normal of the PO_2^- group of DPPC monolayers on the water surface and on the silica substrate calculated from SFG data are found to be 59° ± 3° and 72° ± 5°, respectively. Orientation of the phosphate group is additionally affected by the presence of ions. These findings show that extrapolation of results obtained from model membranes from liquid surfaces to solid supports may not be warranted since there are differences in headgroup organization on the two subphases.

Introduction

Water is critically important in the functioning of biological molecules and their assemblies including membranes. Water-membrane interfaces play a role in fundamental biochemical functions such as the transport of nutrients, protein synthesis, and DNA replication.[1,2] Biological membranes consist of a lipid matrix in which membrane proteins are embedded. These lipids, mainly phospholipids in eukaryotic organisms, are charged entities that are surrounded by an aqueous environment containing ionic species. The properties of these membranes are affected by the electrostatic character of their chemical environment, which includes ionic strength and pH. The interactions between phospholipid membranes and ions play a central role in many biological processes such as neural signal transduction[3] and membrane fusion.[4]

Cations are attracted to the carbonyl groups and the PO_2^- of the phosphate group of phospholipids.[5−9] The interaction between acidic lipids and cations at pH conditions above the pK_a of the headgroup is favored by electrostatic attractions. The interactions of cations with the headgroups of phospholipids are expected to be stronger for negatively charged lipid monolayers such as phosphatidylglycerol compared to those of zwitterionic phosphatidylcholine (PC) monolayers such as dipalmitoylphosphatidylcholine (DPPC). Binding constants of calcium ions to glycerol and PC headgroups were found to be similar in magnitude when corrections for the difference in electric surface potentials were carried out.[10] Moreover, small changes in the headgroup orientation after ion binding was shown to alter the electrical properties of the membrane surface, having an impact on the physiological and biochemical properties of the membrane.[11,12]

The predominant ions surrounding biological membranes include Na^+, K^+, Ca^{2+}, Mg^{2+} and Cl^-.[13] The interactions between monovalent ions and zwitterionic lipids are generally assumed to be somewhat weak. Yet the knowledge of the interaction between monovalent ions and phospholipids is less detailed apart from theoretical work.[13−17] Divalent cations such as calcium ions are known to interact strongly with charged lipids but only moderately with zwitterionic lipids,[5,6,9−11,18−20] yet experimental studies that provide molecular insights of this interaction have also remained limited.[21] Molecular information of this binding process has been explored by theoretical studies, although these reports are usually restricted to a single area per molecule (lipid phase).[9,22,23] Spectroscopic molecular investigations of the binding site, the phosphate group, is required to further elucidate the binding event at different lipid phases.

As an alternative to studying monolayers at the air−water interface, these same monolayers can be transferred to solid supports at different surface pressures. The interactions between membranes and solid surfaces are the subject of study for several industrial and biomedical processes. For instance, there have been studies in toxicity reduction of pyrite[24] and in cell recognition and adherence.[25] These interactions are also important in cell rupture caused by inhaled mineral dust particles in the lungs.[26] Silica particles, particularly crystalline are notoriously toxic and pose serious risk to human health.[27] The molecular mechanism by which cell membranes degenerate upon adhesion of silica particles to the cell surface is still not well understood.[26,28,29]

In this study, we analyze the macroscopic differences from monolayers of DPPC, the most abundant of the pulmonary surfactants,[30] spread on water, NaCl solutions, and $CaCl_2$ solutions using compression isotherms obtained from surface pressure measurements. To study the microscopic differences,

* To whom correspondence should be addressed. E-mail: allen@chemistry.ohio-state.edu.

10.1021/jp1022357
Published on Web 07/08/2010

a surface selective vibrational spectroscopic technique, sum frequency generation (SFG) spectroscopy, was used to examine the hydration and the orientation of the phosphate group of DPPC monolayers at the air-aqueous interface of these three different subphases. Additionally, in an attempt to elucidate the molecular effect of the adhesion of silica particles to cell membranes, we probed the phosphate group of DPPC monolayers supported on silica as a planar membrane model system. The silica-supported DPPC monolayers were transferred from aqueous subphases containing NaCl and $CaCl_2$. Orientation information of the phosphate group of DPPC monolayers at the air−aqueous and air−silica interfaces was also examined.

Experimental Section

Materials. 1,2-Dipalmitoyl-*sn*-glycerol-3-phosphocholine (DPPC) with >99% purity was obtained from Avanti Polar Lipids Inc. (Alabaster, AL) and used without further purification. Spectral grade acetone and chloroform were purchased from Sigma-Aldrich (Allentown, PA). Hellmanex II solution was obtained by Hellma Cells, Inc. (Plainview, NY). Infrared grade fused (amorphous) silica plates of 1.00 in. diameter and 0.188 in. thickness were obtained from Quartz Plus, Inc. (Brookline, NH). All glassware used was cleaned with $(NH_4)_2S_2O_8$ in H_2SO_4 solution (0.08 M) to eliminate trace organics and rinsed with nanopure water from a Barnstead system with a resistivity of 18.2 MΩ·cm.

Sodium chloride (NaCl; ACS certified) and calcium chloride dihydrate ($CaCl_2 \cdot 2H_2O$; ACS certified) were obtained from Fisher Scientific (Pittsburgh, PA). For the sodium chloride solutions, the NaCl salt was placed in a muffle oven (Fisher Scientific, Isotemp Muffle Furnace) at 700 °C for 4 h to eliminate any organic contaminants prior to mixing with nanopure water to obtain the final concentration. For $CaCl_2$, a saturated aqueous solution was prepared and then filtered through a Whatman Carbon-Cap activated carbon filter to remove organic contaminants. The concentration of the filtered $CaCl_2$ solution was determined by the Mohr method.[31] The concentrated $CaCl_2$ solution was then diluted to the final concentration using nanopure water. Salt concentrations in the subphase were chosen to clearly observe SFG signal variation with respect to the neat water subphase.

Methods. ***Substrate Cleaning.*** Amorphous silica plates were cleaned by a series of sonication steps.[32] First, they were sonicated for 15 min in acetone, rinsed in nanopure water, then sonicated for 15 min in 2% Hellmanex II solution, which is an alkaline solution specifically designed to clean quartz cuvettes, then rinsed in nanopure water. Then the plates were sonicated in water for 15 min. Finally, the silica plates were dried in an oven at 70 °C for 10 min. Clean silica plates were analyzed by SFG spectroscopy to verify the absence of CH resonances attributed to organic contaminants.

Langmuir Films. The surface pressure−area isotherms were obtained with a KSV minimicro (KSV, Finland) described in detail elsewhere.[33] The procedure followed to obtain the isotherms has also been described previously.[33] All the isotherms were collected at 22 °C ± 1°.

Langmuir -Blodgett (LB) Films. Langmuir DPPC films were acquired with a minimicro LB-trough from KSV Instruments (Monroe, CT). This trough comprises a dipping well and a linear dipper to transfer the Langmuir film from the aqueous subphase onto the solid substrate. A clean silica plate was clamped onto the dipper and was partially immersed in the dipping well full of the aqueous phase prior to spreading the DPPC film. In the Teflon-coated film trough, a known volume of a 1 mM solution of DPPC in chloroform was spread dropwise on the surface of the water subphase (pH ∼ 6) or aqueous solution. After 10 min to allow for complete solvent evaporation, the compression of the two hydrophilic barriers was initiated. The surface pressure was measured using a Wilhelmy plate composed of Whatman 41 ashless paper. The films were compressed at a constant speed of 5 mm/min. Films were transferred onto the silica substrate by compressing the DPPC film to 40 mN/m followed by withdrawing the silica plate vertically through the interface into the air. The withdrawing speed was 1 mm/min. The surface pressure was maintained at 40 mN/m throughout the deposition process. The temperature for all of the procedures was 22 °C ± 1°. The average transfer ratio measured was ∼1.03 during the transfer process. This film quality parameter is the ratio of the coated area of the solid substrate to the area occupied by the monolayer on the liquid substrate.[34] Silica-coated plates (and uncoated as a control) were analyzed within an hour after film transfer by SFG spectroscopy.

Sum Frequency Generation Spectroscopy. SFG spectra at the air−aqueous and air−silica interfaces were acquired using a broad bandwidth SFG system. Details of the current system can be found in previous publications.[33,35,36] Briefly, two 1 kHz regenerative amplifiers (Spectra Physics, Spitfire, femtosecond and picosecond version) are seeded by a titanium:sapphire oscillator (Spectra Physics, sub-50 fs Tsunami, centered at 792 nm for these studies) and pumped by a Q-switched all solid state Nd:YLF laser (Spectra Physics, Evolution 30 at 527 nm). The femtosecond and picosecond amplifiers produce 85 fs pulses and 2 ps pulses, respectively at 792 nm. The femtosecond output pumps an optical parametric amplifier (OPA) (Light Conversion, TOPAS) to generate a broadband infrared beam of ∼150 cm^{-1} to probe the phosphate region at 1100 cm^{-1}. The output infrared beam is temporally and spatially overlapped with the 792 nm beam from the picosecond amplifier at the surface of the sample to generate the broad band SF beam. The input energies of the broad band infrared beam and the 792 nm beam were 3 and 300 μJ, respectively. A copropagating geometry is used in this SFG system where the incident angles of the infrared and visible from the surface normal were 68° and 53°, respectively. The reflected sum frequency beam is dispersed in a monochromator (Acton Research, SpectraPro 500i) using a 1200 groove/mm diffraction grating blazed at 750 nm (wavelength of maximum efficiency), and then collected in a CCD detection system (Roper Scientific, LN400EB, 1340 × 400 pixel array back illuminated).

Spectra were obtained under the ssp (s for the SFG, s for the 792 nm, and p for the infrared beam) and ppp polarization combinations. SFG spectra were normalized to the nonresonant signal from a GaAs crystal. Detection efficiency differences between the s and p SFG signal were avoided by changing the p-SFG signal to s-SFG signal with a half wave plate just prior to reaching the CCD camera. Spectral calibration was conducted with the absorption bands from a polystyrene film placed in the output port of the OPA when acquiring the nonresonant SFG spectrum from a GaAs crystal. This calibrated SFG system is able to resolve a 1 cm^{-1} peak shift. Fresnel factors are explicitly taken into account in the orientation analysis of the ν_s PO_2^-. For the calculation of the Fresnel factors, the refractive index of the gas, bulk, and the interface should be considered. The gas phase refractive indices were set equal to 1, the refractive index of vacuum. The bulk phase refractive indices were set to 1.33 in the case of water, and 1.45 in the case of silica.[37] For the interfacial region, the refractive index was set equal to 1.18 according to the work reported by Shen and co-workers.[38] In that study, the authors demonstrated that the stated interfacial

refractive index was suitable for the determination of the orientation of amphiphilic molecules forming a Langmuir monolayer on a water surface. An average of at least two replicate spectra is shown in all cases. Spectra were acquired at 22 °C ± 1° and in a range from 30 to 40% relative humidity. Spectra were fit using the software package Igor Pro 4.05. Peak position, peak amplitudes, and peak widths (full width half-maximum, fwhm) were allowed to vary during the fit. Peak positions and peak widths reported are the best fits found with the software.

SFG is a nonlinear vibrational spectroscopic technique that provides surface specific information on conformational order and orientation of interfacial molecules.[33,35,39−45] However, in previous SFG studies of DPPC Langmuir monolayers, researchers have focused mainly on the chain ordering.[21,46,47] Here we focus on the phosphate stretching region at ~1100 cm^{-1}.

A brief description of the SFG theory[48] is presented below. Theory of orientation analysis is presented in the Results Section. The SFG intensity, I_{SFG} is proportional to the absolute square of the macroscopic second order nonlinear susceptibility, $\chi^{(2)}$, which is composed of a nonresonant term $\chi^{(2)}_{NR}$ and a sum of resonant terms $\chi^{(2)}_v$, as shown in eq 1

$$I_{SFG} \propto |\chi^{(2)}|^2 \propto |\chi^{(2)}_{NR} + \sum_v \chi^{(2)}_v|^2 \quad (1)$$

$\chi^{(2)}_v$ is related to the molecular hyperpolarizability, β_v, by the number density of the surface species, N, and an orientationally averaged Euler angle transformation $\langle \mu_{IJK:lmn} \rangle$ between the laboratory coordinates (I, J, K) and the molecular coordinates (l, m, n) as shown in eq 2

$$\chi^{(2)}_v = N \sum_{lmn} \langle \mu_{IJK:lmn} \rangle \beta_v \quad (2)$$

Results and Discussion

In our initial studies, DPPC monolayers spread on aqueous solutions with a range in concentration of 0.1 to 0.5 M of NaCl and $CaCl_2$ were examined. Preliminary results showed that the effect of calcium on the DPPC isotherms was more pronounced than that of sodium. From the aqueous NaCl solutions tested, the greater concentration is presented here to show that even at relatively high concentration of sodium, only a modest effect on the surface organization of phospholipids is observed compared to that of lesser concentrations of calcium.

Isotherms of DPPC. Pressure−area isotherms of Langmuir DPPC monolayers on water, 0.5 M NaCl, and 0.4 M $CaCl_2$ subphases are shown in Figure 1. The isotherms reveal distinct phases that have been previously identified.[33,34] Although differences among the isotherms in Figure 1 are observed with the increase of surface pressure, (obtained from the difference between the surface tension of the pure subphase and with the spread monolayer) the liquid expanded (LE), the coexistence regions between LE and liquid condensed (LC), and the pure LC phases are observed on all the subphases. The gas phase (G) is only observed in the water and the NaCl isotherms.

Investigation of the monolayer on the 0.5 M NaCl solution reveals that the isotherm shifts to slightly higher mean molecular areas (MMAs) in both the LE and the LE−LC regions consistent with other studies.[21,49] The shift has been assigned to the interactions of the sodium ions with the headgroup of the phospholipids inducing disorder in the lipid chains.[21,49,50]

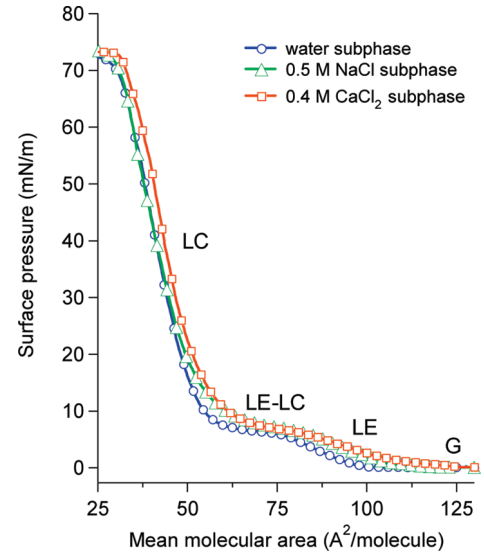

Figure 1. Pressure−area isotherm of DPPC on different subphases; neat water (blue circles), 0.5 M NaCl (green triangles) and 0.4 M $CaCl_2$ (orange squares).

Previously, it has been suggested that the chloride anions are excluded from the headgroup region, particularly around the phosphate group[13,15,22] and are therefore not discussed in this analysis. As the surface pressure increases to the pure LC phase, there is no effect of the sodium ions on the compression isotherm.

With calcium ions in the subphase, a more pronounced shift to higher MMA of the DPPC isotherm is observed at all surface pressures, consistent with previous studies.[21] In the LE phase, similar to the DPPC isotherm with sodium ions, this shift could be the result of calcium ions binding to the headgroup of the phospholipids, providing additional surface area for each DPPC molecule.[21] It has been suggested that at higher surface pressures (~16 mN/m) 1:1 phospholipid/Ca^{2+} complexes are formed leading to a larger MMA by ~4 $Å^2$/lipid. This change in MMA corresponds to the Ca^{2+} ion cross sectional area.[21]Above 16 mN/m the change in MMA is reduced by half (~2 $Å^2$/lipid) suggesting the formation of 2:1 phospholipid/Ca^{2+}complexes.[5,9,21]

In comparing the results for the Ca^{2+} and the Na^+ subphases in the LC region, the phospholipid organization is more affected by Ca^{2+} ions than Na^+ ions, consistent with previous findings.[5,9,21] Surface charge density of Ca^{2+} is approximately twice that of Na^+ given that the ionic radii of Ca^{2+} and Na^+ are similar (100 and 102 pm).[51] Above 16 mN/m in the LC phase, the isotherm from the NaCl subphase overlaps with the purely water subphase. It could be that the Na^+ ions are being squeezed out from the headgroup region. Contrary to the NaCl subphase isotherm, that of the $CaCl_2$ subphase is clearly shifted to larger MMA suggestive of ionic binding to the headgroup.

DPPC Monolayers at the Air−Aqueous Interface. Molecular level information of the interaction and binding of the cations with the phospholipid phosphate headgroups was obtained with SFG spectroscopy. Phosphate groups are likely the most hydrated moieties of phosphatidylcholine molecules within a bilayer.[8,52] Water molecules also interact with the carbonyl groups.[53−55] The water molecules that solvate the phosphate groups form strong hydrogen bonds.[8,52,56,57] Therefore a direct interaction of the cations with the phosphate groups would require the removal of one or more of these solvating water molecules from the cation and the phosphate group. The ability of these ions to lose a portion of their solvation shell ultimately determines the strength of the ion-phosphate interaction.

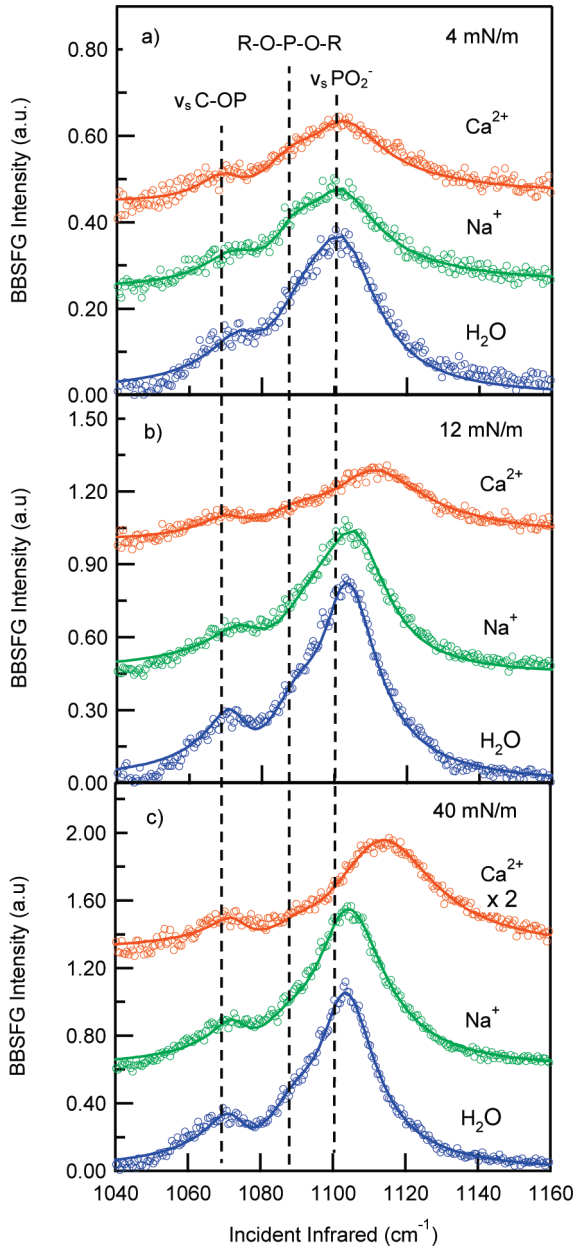

Figure 2. SFG spectra of DPPC monolayers on 0.4 M $CaCl_2$, 0.5 M NaCl, and neat water subphases at (a) 4 mN/m (LE phase), (b) 12 mN/m (LC phase), and (c) 40 mN/m (LC phase) surface pressures.

To elucidate the extent of the cation−phosphate interaction, SFG spectra were obtained from the phosphate group of DPPC monolayers in the presence of sodium and calcium chloride salts. SFG spectra of DPPC monolayers on water, 0.5 M NaCl, and 0.4 M $CaCl_2$ at three surface pressures 4, 12, and 40 mN/m are shown in Figure 2a−c, respectively. These spectra were acquired under the ssp polarization combination. The phases of the DPPC monolayer correspond to the LE at 4 mN/m and to the LC at 12 and 40 mN/m as shown in Figure 1. Two peaks at ∼1070 and 1100 cm^{-1} are observed in all the spectra and are assigned to the phosphate ester stretch C−OP and the symmetric stretch of the PO_2^- (ν_s PO_2^-), respectively.[58,59] The ν_s PO_2^- peak is clearly asymmetric toward the low frequency side, suggesting a third component peak at ∼1090 cm^{-1}, which is assigned to the vibration of the R−O−P−O−R.[60]

After compression from 4 to 40 mN/m of the DPPC monolayers on the three different subphases, a ∼2 cm^{-1} blue shift of the C−OP and the R−O−P−O−R peaks is observed.

TABLE 1: Peak Position and Full Width Half Maximum (fwhm) of the Symmetric Stretch of the PO_2^- Moiety of DPPC Monolayers Spread on Water, 0.5 M NaCl, and 0.4 M $CaCl_2$ Solutions at 4, 12, and 40 mN/m Surface Pressures[a]

		aqueous		silica	
subphase	surface pressure mN/m	PO_2^- peak position cm^{-1}	PO_2^- fwhm	PO_2^- peak position cm^{-1}	PO_2^- fwhm
water	4	1098	40		
0.5 M NaCl	4	1100	44		
0.4 M $CaCl_2$	4	1100	53		
water	12	1103	36		
0.5 M NaCl	12	1103	44		
0.4 M $CaCl_2$	12	1109	61		
water	40	1104	34	1106	24
0.5 M NaCl	40	1104	44	1104	17
0.4 M $CaCl_2$	40	1111	61	1120	36

[a] These same parameters are also shown for the silica-supported DPPC monolayers tranferred at 40 mN/m from the three different subphases.

A significantly larger blue shift of the ν_s PO_2^- peak at ∼1100 cm^{-1} is observed upon compression; yet the extent of this frequency shift is highly dependent on the subphase composition. The blue shift of all these peaks is generally attributed to a difference in the hydration state of the phosphate group at different surface pressures. The smaller shift in frequency observed in the C−OP and the R−O−P−O−R peaks relative to that observed in the ν_s PO_2^- peak is attributed to the fact that the former moieties are solvated more weakly than the PO_2^- moiety.[8] Therefore, to follow the hydration state and ion coordination of the phosphate group in DPPC monolayers, we focus our discussion on the ν_s PO_2^- peak at ∼1100 cm^{-1}. Detailed analysis of these spectra from the DPPC monolayers of the three different subphases is described below and spectral data is summarized in Table 1.

On water, the compression of the DPPC monolayer from 4 to 12 mN/m results in a blue shift of the ν_s PO_2^- peak from 1098 to 1103 cm^{-1}. Further monolayer compression to 40 mN/m results in an additional frequency shift to 1104 cm^{-1}. This shift has been previously attributed to a difference in the hydration state of the phosphate moiety in different structural phases (LE vs LC), where a blue shift is synonymous with dehydration.[33] The reorganization and resultant dehydration of the phosphate has been commonly referred to as a squeezing out of the water molecules. In the LE phase, the loosely packed phosphate groups of the DPPC molecules are well solvated; however as the DPPC molecules are compressed to the LC phase, the water molecules of the phosphate's hydration shell reorganize and decrease in number (on average moving away from the phosphate) and, hence, dehydration of the phosphate group occurs. Even within the LC phase (at 12 and 40 mN/m), different hydration states of the phosphate are observed. This is because at 12 mN/m the DPPC molecules are not completely condensed since further compression of the monolayer is possible. A shift in frequency attributed to a change in the hydration state of the phosphate moiety has also been reported in IR spectroscopic studies of DPPC.[61−63] From the perspective of hydration, theoretical studies of the PO_2^- moiety of methylphosphocholine have shown that upon hydration there is a loss of electron density of the P−O bonds due to strong hyperconjugation with the O−H antibonding orbital of water that then weakens the P−O bond resulting in a red shift.[64] This finding is consistent with our compression studies showing a blue shift with dehydration. It has been reported that the number of water molecules in the interfacial

region changes from ~9 per DPPC in the liquid crystalline phase (corresponding to the LE phase in a monolayer) to ~4 per DPPC in the gel phase (analogous to the LC phase in a monolayer).[65] These remaining four water molecules are expected to be associated with the hydrophilic moieties including the phosphate. That is, a complete removal of water molecules from the headgroup is unlikely.

In addition to the frequency shift, we also observe a change in the full width half-maximum (fwhm) of the ν_s PO_2^- peak, which decreases as a result of the monolayer compression. From peak fitting, the fwhm of the ν_s PO_2^- peak from the water subphase at 4, 12, and 40 m N/m is determined to be 40, 36, and 34 cm^{-1}, respectively.

In the presence of sodium in the aqueous subphase (0.5 M NaCl), SFG spectra obtained upon compression of the DPPC monolayer also reveals shifts of similar magnitude to the water subphase spectra, suggesting a similar hydration environment of the phosphate group in the presence of sodium with the exception of the spectrum obtained in the LE phase. In this LE phase, the PO_2^- peak is blue shifted with respect to that obtained in pure water suggesting dehydration likely due to sodium. At higher surfaces pressures, in addition to dehydration caused by compression of the monolayer, the sodium ions are not perturbing the phosphate moiety to a significant extent, suggesting that the ions are not binding strongly to the PO_2^-. Upon examination of the fwhm, we observe significant differences for the spectra of aqueous sodium versus purely water subphases. Unlike on the water subphase where narrowing of the spectra is observed with compression, the fwhm of the ν_s PO_2^- peak remains constant at ~44 cm^{-1}, indicating a broader distribution of solvation environments for the sodium subphase monolayer. This may be also due to a broader distribution of the orientation of the phosphate moieties in the presence of sodium as well as to vibrational relaxation effects and therefore changes in the lifetime of the transition. Additionally, an increase in the structural heterogeneity of the hydrated phosphate as induced by sodium may lead to a larger fwhm. Although we do not observe a frequency shift with sodium relative to the pure water subphase in the LC phase, the significant changes in the fwhm indicate that sodium ions do perturb the phosphate group and therefore the monolayer. This perturbation may include an alteration of the ordered water molecules adjacent to the DPPC headgroup[66] due to the concentration gradient of ions[13,15,22] in this region.

The findings above are consistent with recent molecular dynamics studies of DPPC bilayers that have shown that sodium interacts with the phosphate group creating complexes with several DPPC molecules at surface pressures of ~10 mN/m.[15−17] It has been suggested that the sodium ions lose part of their first solvation shell water molecules to interact with the hydrated phosphate group.[15−17] However, the binding constants of Na^+ to the phosphate group have been estimated to be relatively weak in a range from 0.15 to 0.61 M^{-1},[15,67,68] suggesting ion exclusion at high surface pressures.[49] The presence of sodium in the subphase also has been reported to slightly affect alkyl chain conformation of DPPC monolayers at high surface pressures.[21]

In brief, from the studies presented here, the presence of sodium chloride in the subphase causes a perturbation of the phosphate group of the DPPC monolayers. At lower surface pressures, binding of the sodium ion to the phosphate group is suggested. As the DPPC monolayer is compressed, only a slight perturbation of the phosphate group is suggested.

The SFG spectra of the DPPC monolayer in the presence of calcium (0.4 M $CaCl_2$) are remarkably different than those observed in the absence of ions (neat water) and in the presence of sodium as shown in Figure 2. The hydration environment of the phosphate moiety is affected by the monolayer organization in different structural phases, and also by the binding of calcium to the phosphate group. In the LE phase as shown in Figure 2a, a similar peak position of the ν_s PO_2^- peak is observed from all the subphases, although clear differences in the fwhm are revealed (Table 1).

Upon compression of the DPPC monolayer to 12 mN/m in the presence of calcium, the ν_s PO_2^- peak is ~6 cm^{-1} blue shifted with respect to the peaks observed in water and in the presence of sodium. This suggests that calcium binding results in phosphate group dehydration. This is consistent with exclusion of the water molecules from both the phosphate group and the calcium hydrate upon binding.[69,70] This is in stark contrast to the sodium cations that bind to hydrated phosphate groups, as shown here and discussed by others.[15−17] The stronger attraction between calcium and the phosphate groups compared to that between sodium and the phosphate groups is consistent with the reported binding constants for these ions to the phosphatidylcholine groups as well. The binding constant for calcium was estimated to be in a range from 12 to 37 M^{-1},[10,11,67] which is 2 orders of magnitude larger than that reported for sodium (see above). At higher surface pressure (40 mN/m), the ν_s PO_2^- peak is 2 cm^{-1} blue shifted relative to that obtained at 12 mN/m suggesting a larger exclusion of water molecules from the phosphate group as more calcium ions are bound. These results are in agreement with previous reports that suggest that the binding constant of calcium ions to the phosphate moiety is dependent on the phase state of the lipid bilayers (gel state > pretransition state > liquid state).[71]

The observed spectral blue shift of the ν_s PO_2^- peak is consistent with theoretical studies on dimethyl phosphates in the presence of water and calcium that have shown that as the calcium cation approaches the anionic oxygens, a blue shift of the symmetric mode of the PO_2^- is observed.[69] The internal geometry of dimethyl and dihydrogen phosphates has been reported to be sensitive to the counterion position.[72] Then it is expected that upon direct calcium binding the symmetry of the phosphate group is modified to some degree. This argument could also be applied when sodium ions are present in the subphase; however the extent of this perturbation is expected to be smaller because water molecules mediate the coordination between the phosphate group and the sodium ions.

Larger fwhm values of the ν_s PO_2^- peaks compared to those on water and with sodium present were observed at all surface pressures. With calcium present, the fwhm of the ν_s PO_2^- peak changes from 53 cm^{-1} in the LE phase to 61 cm^{-1} in the LC phase at 12 and 40 mN/m as observed in Figure 2. These larger fwhm can be attributed to a broader distribution of the orientation of the phosphate group and therefore an increase in the structural heterogeneity of the phosphate-calcium complexes formed in all lipid phases.

The hydration environment of the phosphate group may be also affected by the calcium concentration available in the subphase, particularly at the interface. In Figure 3, the SFG spectra of the DPPC monolayers at 40 mN/m in the presence of 0.1 and 0.4 M $CaCl_2$ in the subphase are shown. The SFG spectra of a DPPC monolayer spread on water is also shown for reference. These spectra reveal that as the Ca^{2+} concentration increases, a larger blue shift of the ν_s PO_2^- peak is observed. This suggests that a larger number of the phosphate groups are bound to Ca^{2+} with the increased availability of Ca^{2+} in the aqueous phase. Also observed is a difference in the signal

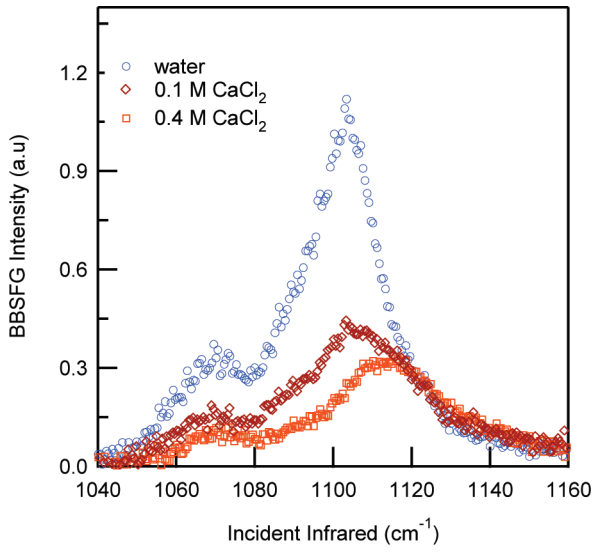

Figure 3. SFG spectra of DPPC monolayers on 0.1 and 0.4 M $CaCl_2$ obtained at 40 mN/m. SFG spectra of a DPPC monolayer on water at 40 mN/m is also shown for reference.

intensity of the ν_s PO_2^- peak in both calcium solutions relative to the purely water subphase. This intensity decrease is likely due to a convolution of two factors, a change in the average orientation of the phosphate group as Ca^{2+} cations are bound, and a variation of the extinction coefficient of the PO_2^- group when the PO_2^--Ca complex is formed.[69]

In the analysis of the spectra presented in Figures 2 and 3, a clear increase in the signal intensity is observed as the DPPC monolayers are compressed in all the three subphases. However, sum frequency intensity is proportional not only to the number density (N^2), but also to the mean molecular orientation. Below, the orientation of the phosphate group of a DPPC monolayer spread on neat water in the LC phase is analyzed in detail.

The orientation of the DPPC phosphocholine headgroup, which is related to the structure of the interfacial phospholipid monolayer, has been the subject of study in previous reports.[9,15,17,73−78] Nonetheless, these studies are mainly theoretical efforts. Because of the lack of experimental techniques able to determine the headgroup orientation, there is a dearth of experimental evidence to support or refute the theoretical data. An SFG polarization study could offer headgroup orientation because of its capability of providing quantitative orientation values given certain theoretical treatments. To this aim, the ppp polarized spectra of a DPPC monolayer on water at 40 mN/m surface pressure was obtained in the phosphate region (~1100 cm^{-1}). Both ssp and ppp spectra were acquired with the same geometrical configuration (incident angles) of the incoming laser beams. This SFG ppp spectrum, and under the ssp polarization for reference, are shown in Figure 4a.

The experimentally measured SFG intensity in different polarization combinations is related to macroscopic orientational average $\chi_v^{(2)}$, through the microscopic molecular polarizability tensor beta β_v (as shown in eq 2) and the symmetry of the group. The PO_2^- moiety on the DPPC headgroup can be treated as having C_{2v} symmetry. The effective nonlinear susceptibility $\chi_{eff}^{(2)}$, under the ssp and ppp polarization combinations are expressed as follows[79]

$$\chi_{eff,ssp}^{(2)} = L_{yy}(\omega)L_{yy}(\omega_1)L_{zz}(\omega_2)\sin\beta_2\chi_{yyz}$$

$$\begin{aligned}\chi_{eff,ppp}^{(2)} = &-L_{xx}(\omega)L_{xx}(\omega_1)L_{zz}(\omega_2)\cos\beta\cos\beta_1\sin\beta_2\chi_{xxz}\\ &-L_{xx}(\omega)L_{zz}(\omega_1)L_{xx}(\omega_2)\cos\beta\sin\beta_1\cos\beta_2\chi_{xzx}\\ &+L_{zz}(\omega)L_{xx}(\omega_1)L_{xx}(\omega_2)\sin\beta\cos\beta_1\cos\beta_2\chi_{zxx}\\ &+L_{zz}(\omega)L_{zz}(\omega_1)L_{zz}(\omega_2)\sin\beta\sin\beta_1\sin\beta_2\chi_{zzz}\end{aligned} \quad (3)$$

where L represents the tensional Fresnel factors at the frequency, ω is for the SFG, ω_1 is for the visible, ω_2 is for the infrared, and β_i's only in eq 3 are the angles of the beams. χ_{xxz} and χ_{zzz} can be further described as

$$\begin{aligned}\chi_{xxz} &= \chi_{yyz}\\ &= \frac{1}{2}N[(\cos^2\psi)\beta_{aac} + (\sin^2\psi)\beta_{bbc} + \beta_{ccc}](\cos\theta) +\\ &\quad \frac{1}{2}N[(\sin^2\psi)\beta_{aac} + (\cos^2\psi)\beta_{bbc} - \beta_{ccc}](\cos^3\theta)\end{aligned}$$

$$\begin{aligned}\chi_{zzz} = &N[(\sin^2\psi)\beta_{aac} + (\cos^2\psi)\beta_{bbc}](\cos\theta) -\\ &N[(\sin^2\psi)\beta_{aac} + (\cos^2\psi)\beta_{bbc} - \beta_{ccc}](\cos^3\theta)\end{aligned} \quad (4)$$

θ is the average tilt angle of PO_2^- group to the surface normal, ψ is the average twist angle of the PO_2^- group about its molecular c axis as shown in Figure 5a. Previous studies have made different assumptions on the value of ψ based on the different molecular structures.[79] In general, the liquid surface is considered to be isotropic, hence the azimuth angle (rotation about lab z-axis) is averaged out from 0 to 360°. In this study, due to the upward orientation of the DPPC alkyl chains (and therefore the constrained orientation of the headgroup), the twist of the PO_2^- groups is hindered by neighboring atoms on the same molecule. Therefore, it is reasonable to constrain the twist angle to a small value. Here we assume that the angle approaches zero. From this analysis, and if the tilt angle is large enough, like it is expected in the PO_2 case,[59] the twist angles also are assumed to have a narrow distribution.[80]

Given the value of molecular polarizability tensors, the average orientation of the PO_2^- group is obtained through the SFG intensity ratio of ssp to ppp. Previous SFG studies have demonstrated that the ratio of β can be determined through the experimentally measured Raman depolarization ratio ρ. For C_{2v} symmetry, it is described by

$$\rho = \frac{3}{4 + 20\dfrac{(1+2r)^2}{(1-r)^2(1+3\cos^2\tau)}} \quad (5)$$

where r is the single bond polarization derivative ratio and τ is the angle between the two bonds (angle O−P−O) in C_{2v}

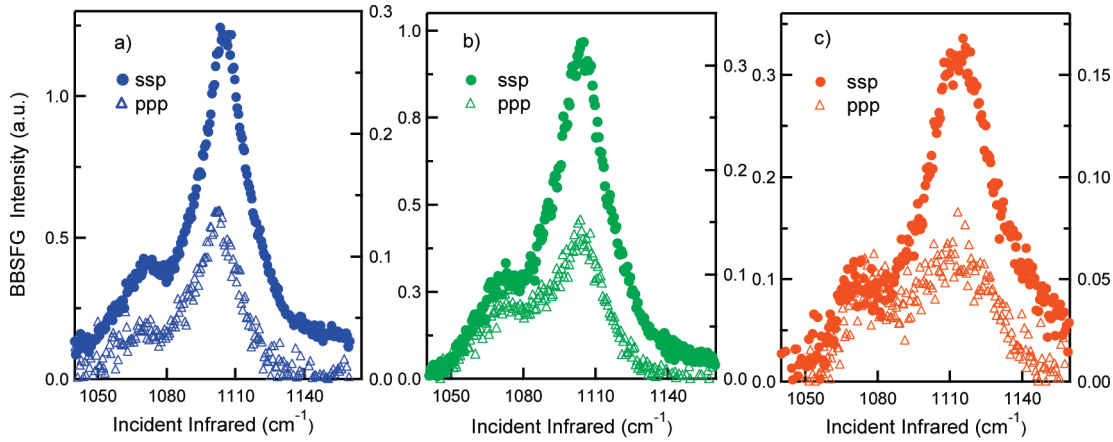

Figure 4. SFG spectra under ssp and ppp polarization combinations of DPPC monolayers on (a) water, (b) 0.5 M NaCl, and (c) 0.4 M $CaCl_2$ subphases at 40 mN/m surface pressure (LC phase).

symmetry. On the basis of bond polarization derivative ratio model, the ratio of β can be expressed as

$$\frac{\beta_{aac}}{\beta_{ccc}} = \frac{(1+r)-(1-r)\cos\tau}{(1+r)+(1-r)\cos\tau}$$

$$\frac{\beta_{bbc}}{\beta_{ccc}} = \frac{2r}{(1+r)+(1-r)\cos\tau} \qquad (6)$$

With the value of the measured Raman depolarization ratio 0.05 with a τ of 120° reported for dimethyl phosphate,[81] we calculate the ratio of the molecular polarizability tensors, hence the average tilt angle, θ, of PO_2^-. The calculated tilt angle of the PO_2^- of DPPC monolayers in the water surface is found to be 59° ± 3° from the surface normal (this uncertainty originates from the dispersion in the experimental data). A variation of ±10% of the Raman depolarization ratio (RDR) value leads to a change in the tilt angle of the PO_2^- of ±7% showing the sensitivity of the tilt angle to the RDR used. In addition, a variation of the twist angle, Ψ, to ±10° causes a change in the average orientation of the PO_2^- of ±8°. Our tilt angle value is within the range of previous results from IR studies of DPPC bilayers that reported 56°.[59,82]

In the presence of sodium and other divalent cations, the angle of O−P−O in dimethyl and dihydrogen phosphates is affected;[72] similar changes would be expected in the phosphate moiety of DPPC. As shown in eqs 5 and 6, a variation in τ would have an impact in the determination of the PO_2^- tilt angle. Additionally, after the addition of cations to the water subphase a positive charge in the membrane of vesicles has been observed.[67] This change in the electrical properties of the membrane would have an impact on its optical properties particularly the refractive index. However, if one assumes that the change in τ is negligible, and that the symmetry of the phosphate group and that the refractive index at the interface have not changed significantly, the PO_2^- tilt angle of DPPC on the salt solutions can be determined from the spectra shown in Figure 4b,c. The PO_2^- tilt angle on the sodium subphase was calculated from the surface normal to be 64° ± 2° as compared to that on water, 59° ± 3°. However, the calculation for DPPC on the $CaCl_2$ solution did not provide a physically reasonable ratio, confirming that the assumptions in this case were flawed. Another reason for this analysis to be faulty is if upon ion binding the orientation angle distribution becomes bi or trimodal.

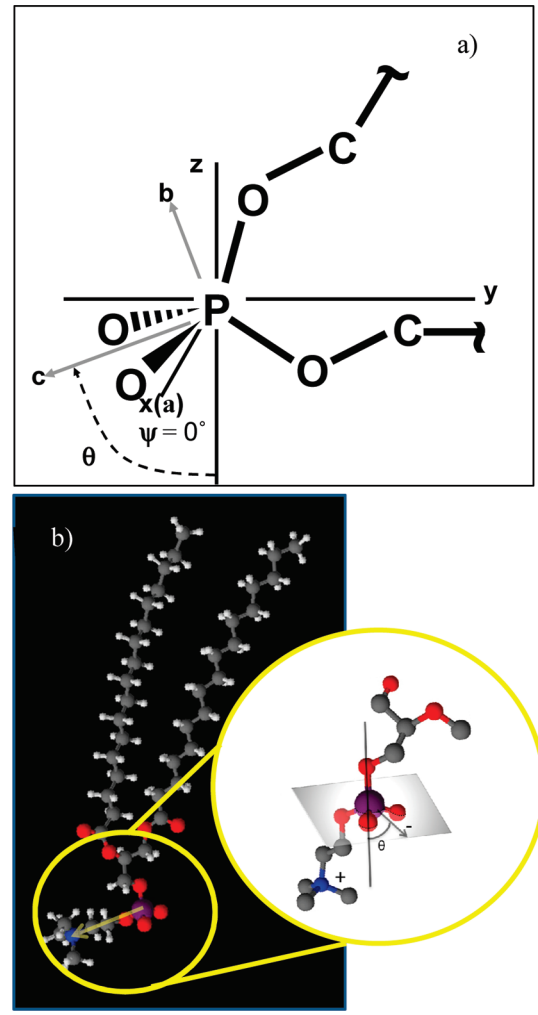

Figure 5. Graphical representation of (a) the molecular and laboratory axes, *a*,*b*,*c* and *X*, *Y*, *Z*, respectively of the phosphate group where the *a* and *X* axes are chosen to be overlapped. The tilt angle, θ which is considered to be between *Z* and *c*, and the twist angle,Ψ which is considered to be zero, are also shown. In (b) the DPPC molecule showing the phosphate−nitrogen vector with a yellow arrow and the tilt angle, θ of the phosphate group in the inset is shown with a smaller gray arrow. The carbon, oxygen, phosphorus, nitrogen, and hydrogen atoms are represented by gray, red, purple, blue, and white spheres, respectively.

The orientation or tilt angle of the headgroup of phosphatidylcholine is usually referred to as the angle between the vector

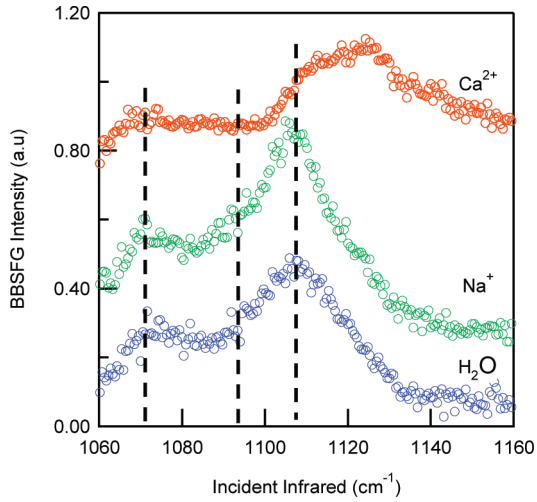

Figure 6. SFG spectra of DPPC monolayers on silica at 40 mN/m transfer pressure from water, 0.5 M NaCl, and 0.4 M $CaCl_2$ subphases.

connecting the phosphorus atom and the nitrogen atom (P−N vector, Figure 5b) with respect to the surface normal.[9,15,17,74,75,77,78] Theoretical studies of DPPC bilayers have shown that the angle of the P−N vector changes in the presence of halide salts compared to that in pure water.[9,13,23,77] Calcium ions were shown to have a larger effect on the angle of the P−N leading to smaller angles from the surface normal. In general, the presence of both sodium and calcium ions leads the P−N vector to lie more outward from the membrane (smaller angles from the surface normal). Although the PO_2^- tilt angle, as calculated here, provides information on the DPPC headgroup, the headgroup itself is better described by the P−N vector. Additionally, changes in the conformation of the headgroups of DPPC bilayers and monolayers have been described in theoretical and experimental studies in different phases.[73,76] These studies have shown that the P−N dipole of the DPPC headgroup exhibits an in-plane orientation with respect to the monolayer in the LE phase (liquid crystal in the bilayer), and a more tilted orientation is found in the LC phase (gel phase in the bilayer). Thus, based on these studies and the results presented here a change in the orientation of the phosphate group is expected upon ion binding.

DPPC Monolayers at the Air−Silica Interface. To examine the interactions of the headgroup of DPPC monolayers with the silica surface, Langmuir−Blodgett (LB) films deposited on amorphous silica were obtained and then analyzed by SFG spectroscopy. SFG spectra of the air−silica interface after the deposition of DPPC monolayers in the phosphate region were acquired under the ssp polarization combination and are shown in Figure 6. These DPPC films were transferred at a surface pressure of 40 mN/m from water, 0.5 M NaCl, and 0.4 M $CaCl_2$ subphases.

Similar to the air-aqueous SFG spectra shown in Figure 2c, the SFG spectra at the air−silica interface in Figure 6 reveal three main peaks which have spectral positions that are highly dependent on the composition of the subphase where the monolayers were transferred from. Spectra from clean silica plates were also acquired (spectra not shown) as control experiments and no SFG signal was detected.

In the SFG spectra from the silica-supported DPPC monolayer transferred from a water subphase, the C−OP and the R−O−P−O−R peaks are observed at 1073 and 1090 cm^{-1}, respectively. These peak positions are almost identical to those obtained from the water subphase at 40 mN/m (Figure 2c) at 1072 and 1090 cm^{-1}. The ν_s PO_2^- peak is found at 1106 cm^{-1} which is 2 cm^{-1} blue shifted (suggesting dehydration) relative to that on water suggesting a slightly different hydration state of the phosphate group of DPPC at the silica surface. In the presence of sodium, the ν_s PO_2^- peak position from the silica supported monolayer and the aqueous sodium subphase is the same. Whereas in the presence of calcium, the peak position differs by 9 cm^{-1} for the silica-supported monolayer (1120 cm^{-1}) versus that in the aqueous calcium (1111 cm^{-1}) subphase. Also different are the fwhm values of the PO_2^- peak from the silica-supported DPPC monolayers where the fwhm value ranges from 10 to 35 cm^{-1} smaller than those found on the aqueous subphases, indicating a different hydration environment of the phosphate group and possibly a narrowing of the orientation distribution on the silica-supported subphases. Another reason for this could be slower reorientation dynamics and vibrations arising from a more homogeneous environment. Differences in the signal intensity of the PO_2^- peak of the monolayer spread on the aqueous and on silica-supported subphases are observed; these are in part due to the differences in Fresnel factors and orientation of the phosphate group. Organization of the alkyl chains in both the water subphase and the silica substrate revealed minimal differences at this surface pressure (spectra not shown). To summarize, it is suggested that the phosphate moiety of DPPC is affected by the presence of the silica surface as shown by the comparison of peak positions and fwhm values with those found in the monolayers spread in aqueous solutions (Table 1). A more detailed analysis of the silica supported DPPC monolayers in the absence (neat water) and in the presence of sodium and calcium is provided below.

As previously described, the phosphocholine headgroup is sensitive to the electric surface charge and dipole fields.[12] The surface charge on silica emanates from the protonation−deprotonation of surface silanol groups and has already been studied in great detail.[83,84] The pH at the point of zero charge (pH_{pzc}) reported for amorphous silica ranges from 2 to 3.5.[83,85,86] Therefore, the amorphous silica surface is negatively charged under the experimental condition of this study since the water pH > pH_{pzc}. Even on a negatively charged surface, the majority of the surface groups expected are the neutral silanol groups, that is, the Si−OH groups.[87] Precisely these silanol groups could form hydrogen bonds with the phosphate groups causing a perturbation of the hydration environment of the phosphate moiety seen as a blue shift of the ν_s PO_2^- peak. This hydrogen bond formation has been previously suggested by Chunbo et al. in NMR studies of DPPC liposomes and silica particles.[88] Yet for the formation of these hydrogen bonds, it is the water molecules present between the silica surface and the headgroup of DPPC[89,90] that are responsible for maintaining the membrane fluidity in solid-supported systems[91] that would need to be displaced.

At this near-neutral pH, there is a relative absence of orientational order of water molecules induced by the surface charge of silica as shown by our earlier work[40] and by others.[42,92,93] The dipole potential of the headgroup of the DPPC molecules leads to an ordering of adjacent water molecules.[66] Consequently, the trapped thin water layer is likely to be highly structured, which can alter the headgroup hydration[94] (studies are underway in our laboratory). In fact, recent molecular dynamics simulations of 1-palmitoyl-2-oleoyl-*sn*-glycero-3-phosphocholine (POPC) bilayers interacting with amorphous silica have shown that this water layer lacks bulklike properties and is thin enough to consist only of bound waters hydrating the lipid head groups and the hydrophilic silica surface.[95] Then

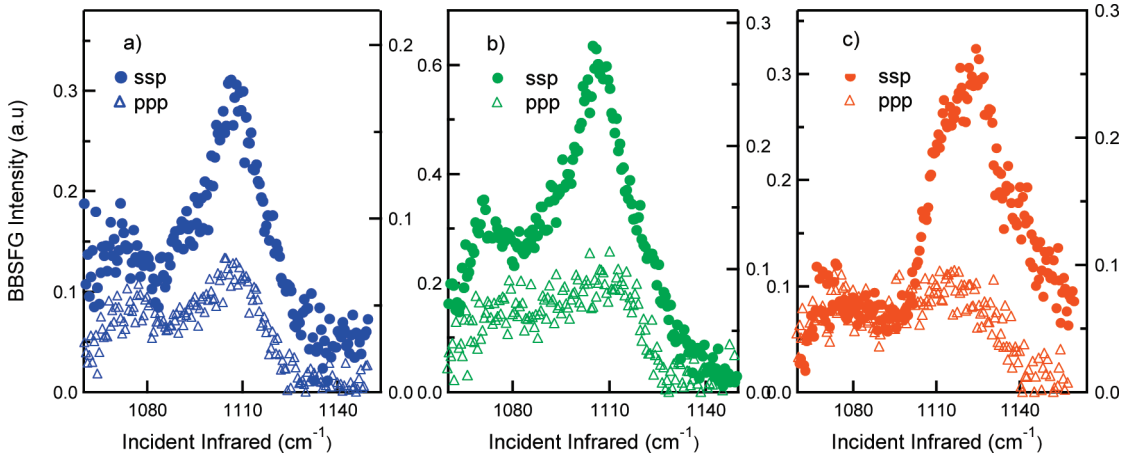

Figure 7. SFG spectra under ssp and ppp polarization combinations of DPPC monolayers on silica transferred from (a) water, (b) 0.5 M NaCl, and (c) 0.4 M $CaCl_2$ at 40 mN/m transfer pressure.

the interaction of the phosphate group of the DPPC monolayers with the silica surface take place through highly structured water molecules adjacent to the silica surface leading to a relatively dehydrated headgroup.

The interaction of the silica surface with the headgroup of DPPC could also involve electrostatic interactions between the positively charged choline groups with negatively charged $Si-O^-$ groups. Studies of bulk adsorption isotherms of DPPC vesicles on quartz at 55 °C have suggested that the electrostatic interactions between these groups are negligible compared to interaction between the phosphate group and the silica surface.[96] This was attributed to the lower positive charge density associated to the choline group compared to the negative charge density associated to the phosphate moiety.[96] The lipid adsorption affinity to the silica surface is not modified or altered by the phase of the lipid.[97] NMR studies have reported that the choline group mobility of DPPC decreases after interacting with quartz[98] suggesting a weak electrostatic interaction between the quartz surface and the headgroup of DPPC. In brief, the hydration environment of the phosphate group is affected in the silica-supported DPPC monolayers as seen by a change in the peak position and fwhm of the PO_2^- peak.

With sodium present (Figure 6), the SFG spectrum of the silica-supported DPPC monolayer shows an identical spectral position of the C−OP and the R−O−P−O−R peaks as those of the DPPC monolayer transferred from a water subphase. Comparison of the silica-supported DPPC monolayer in the presence and absence of sodium is discussed below. As stated above, the ν_s PO_2^- peak is found at 1104 cm^{-1} which is 2 cm^{-1} red shifted relative to that from water (1106 cm^{-1}), and the fwhm of the ν_s PO_2^- peak in the presence of sodium is ~10 cm^{-1} smaller than that found from a water subphase suggesting a perturbation of the phosphate group in the presence of sodium. This is consistent with the differences observed in the aqueous subphases in the presence of sodium (Figure 2). The sodium ions are known to interact electrostatically with the negatively charged $Si-O^-$ groups[99] screening its surface charge, and also promoting negative surface charge density by deprotonating the Si−OH groups.[100] Induced orientational order of water molecules near the silica surface in the presence of NaCl has been reported at the pH of these studies.[101,102] As discussed above, the headgroup dipole potential leads to an ordering of the solvating water molecules.[66] As a result, the trapped thin aqueous layer between the silica surface and the headgroup of the DPPC monolayer is likely to be structured as described for the case in the absence of salts. Interestingly the ν_s PO_2^- peak in the silica-supported monolayer exhibits the same spectral position as that found in the 0.5 M NaCl solution subphase (Figure 2c), suggesting a similar hydration environment of the phosphate group. It is suggested that in general the phosphate group hydration is not strongly affected by the surface charge of the silica surface in the presence of sodium ions.

The SFG spectrum of the silica-supported DPPC monolayer in the presence of calcium ions reveals similar peak positions of the C−OP and the R−O−P−O−R peaks as those found in the absence of ions (pure water/silica, Figure 6). The PO_2^- peak however reveals a significant blue shift of 12 cm^{-1} relative to that found on pure water/silica. Also, this peak is 9 cm^{-1} blue shifted relative to that found from the 0.4 M $CaCl_2$ subphase (Figure 2c), suggesting a different hydration environment of the phosphate moiety in both subphases (aqueous Ca^{2+} vs aqueous Ca^{2+}/silica). Differences in the fwhm values in the presence of calcium and in neat water are observed on the silica-supported DPPC monolayers, as observed in the case of the aqueous solutions (Figure 2). Similar to the case of sodium, water orientation near the silica surface and promotion of the negative surface charge density are expected when calcium ions are present.[100,103] This surface charge increment is greater compared to that induced by sodium,[100] consequently the induced order of the water molecules by the surface charge is expected to be greater. Upon calcium binding to the phosphate groups the zwitterionic nature of the DPPC molecules is perturbed and the generation of a positive charge is expected on the monolayer surface, similar to the increase in the ζ-potential observed on DPPC liposomes studies in the presence of calcium.[67] The water layer hydrating the silica surface, the headgroups, and the calcium ions is believed to be more structured than that observed in the presence of sodium ions and in the absence of ions and is consistent with our work (SFG spectra not shown). This results in dehydrated phosphate moieties in the proximity of the silica surface under these experimental conditions.

Orientation of the PO_2^- moiety of the headgroup of silica-supported DPPC monolayers was obtained using the SFG intensity ratio of ssp to ppp as previously described. SFG spectra of a silica-supported DPPC monolayer are shown in Figure 7. The calculated average tilt angle from the surface normal of the PO_2^- of DPPC monolayers supported on silica is found to be 72° ± 5°, which is 13° larger than that from the water subphase. This indicates that the PO_2^- vector is oriented more in the plane of the silica surface when the DPPC monolayer is supported on that surface. As indicated previously, by making

assumptions in the case of the aqueous Na^+/silica the PO_2^- tilt angle is calculated to be 42°. The calculation from the intensity ratio from the Ca^{2+}/silica did not produce a physically reasonable tilt angle, similar to the case of the aqueous Ca^{2+} subphase. Because of the assumptions made, we are cautious about these estimated numbers; however, the change in PO_2^- tilt angle from water/silica and aqueous Na^+/silica is consistent with the picture of more and more ions being bound to the phosphate moiety, modifying the PO_2^- tilt angle relative to the surface normal.

Differences in the orientation angle of the $N-(CH_3)_3^+$ of the choline group of 1,2-distearoyl-*sn*-glycero-3-phosphocholine (DSPC) bilayers in contact with the silica surface and in contact with the aqueous phase have been reported by Liu et al.[104] In the Liu study, the choline group vector was shown to be oriented more in the bilayer plane when the DSPC bilayer was in contact with the silica surface. Additionally, other effects have been described in computational studies. For instance, ab initio calculations performed by Murashov et al[105] revealed that dihydrogen and dimethyl phosphate anions showed a reduction of the COPO torsion angle upon coordination with orthosilicic acid. Also molecular dynamic simulation of 1-palmitoyl-2-oleoyl-*sn*-glycero-3-phosphocholine (POPC) bilayers showed that diffusion of lipids in the monolayer having direct contact with the silica surface is substantially reduced even under conditions where no structural change of the alkyl chains is observed.[95] The same conclusion was drawn from NMR studies of DPPC bilayers supported on silica.[106] From the studies presented here, we find that both the hydration environment and the orientation of the phosphate moiety of a DPPC monolayer is affected considerably at the silica surface compared to that in contact with the aqueous subphase.

Conclusions

Results from hydration and orientation studies of the phosphate moiety from DPPC monolayers on water, aqueous Na^+, and aqueous Ca^{2+} subphases were compared to each other and to studies of silica-supported DPPC monolayers in the absence (pure water) and in the presence of Na^+ and Ca^{2+}. The PO_2^- moiety from the DPPC headgroup was observed to undergo dehydration with increasing surface pressure and additional dehydration environments from the interactions with Na^+ and Ca^{2+} ions. Ca^{2+} was observed to bind effectively to the PO_2^- of the phosphate group in the aqueous and in the silica-supported studies, although Na^+ also showed some evidence of binding, albeit water mediated. Significant differences in fwhm from the spectra of the hydrated silica surface were observed, revealing varied hydration environments in the silica-supported systems, particularly in the presence of Ca^{2+}. Moreover, the larger differences in the PO_2^- tilt angles from the water and aqueous salt versus the silica-supported systems reveal influence of the silica support modified strongly by the presence of salt. This finding additionally provides information that may be relevant with respect to understanding the pathogenicity of silica in pulmonary systems. In summary, the binding of ions to the headgroup of lipids is affected by the solid support. Moreover, the results presented here show that one needs to be careful when extrapolating model membranes from liquids to solid supports since differences in the organization of the headgroup occur.

Acknowledgment. This research is supported by the U.S. Department of Energy, Office of Basic Energy Sciences, Division of Chemical Sciences, Geosciences, and Biosciences, and the National Science Foundation, NSF-CHE.

References and Notes

(1) Knepp, V.; Guy, R. H. *J. Phys. Chem. B* **1989**, *93*, 6817.
(2) *Biomembranes*; Gennis, R. B., Ed.; Springer: New York, 1989.
(3) *Molecular biology of the cell*; Alberts, B.; Johnson, A.; Lewis, J.; Raff, M.; Roberts, K.; Walter, P., Eds.; Garland Science: New York, 2002.
(4) Szule, J. A.; Jarvis, S. E.; Hibbert, J. E.; Spafford, J. D.; Braun, J. E. A.; Zamponi, G. W.; Wessel, G. M.; Coorssen, J. R. *J. Biol. Chem.* **2003**, *278*, 24251.
(5) Altenbach, C.; Seelig, *J. Biochemistry* **1984**, *23*, 3913.
(6) Binder, H.; Zschörnig, O. *Chem. Phys. Lipids.* **2002**, *115*, 39.
(7) Herbette, L.; Napolitano, C. A.; McDaniel, R. V. *Biophys. J.* **1984**, *46*, 677.
(8) Lopez, C. F.; Nielsen, S. O.; Klein, M. L.; Moore, P. B. *J. Phys. Chem. B* **2004**, *108*, 6603.
(9) Vernier, P. T.; Ziegler, M. J.; Dimova, R. *Langmuir* **2009**, *25*, 1020.
(10) Seelig, J. *Cell. Biol. Int. Rep.* **1990**, *14*, 353.
(11) Akutsu, H.; Seelig, J. *Biochemistry* **1981**, *20*, 7366.
(12) Seelig, J.; Macdonald, P. M.; Scherer, P. G. *Biochemistry* **1987**, *26*, 7535.
(13) Böckmann, R. A.; Hac, A.; Heimburg, T.; Grubmüller, H. *Biophys. J.* **2003**, *85*, 1647.
(14) Berkowitz, M. L.; Bostick, D. L.; Pandit, S. *Chem. Rev.* **2006**, *106*, 1527.
(15) Pandit, S. A.; Bostick, D.; Berkowitz, M. L. *Biophys. J.* **2003**, *84*, 3743.
(16) Pandit, S. A.; Bostick, D.; Berkowitz, M. L. *Biophys. J.* **2003**, *85*, 3120.
(17) Sachs, J. N.; Nanda, H.; Petrache, H. I.; Woolf, T. B. *Biophys. J.* **2004**, *86*, 3772.
(18) *Phospholipids handbook*; Cevc, G., Ed.; Marcel Dekker, Inc: New York, 1993.
(19) Mattai, J.; Hauser, H.; Demel, R. A.; Shipley, G. G. *Biochemistry* **1989**, *28*, 2322.
(20) Uhríková, D.; Kucerka, N.; Teixeira, J.; Gordeliy, V.; Balgavy, P. *Chem. Phys. Lipids* **2008**, *155*, 80.
(21) Sovago, M.; Wurpel, G. H.; Smits, M.; Müller, M.; Bonn, M. *J. Am. Chem. Soc.* **2007**, *129*, 11079.
(22) Böckmann, R. A.; Grubmüller, H. *Angew. Chem., Int. Ed.* **2004**, *43*, 1021.
(23) Cordomí, A.; Edholm, O.; Perez, J. J. *J. Phys. Chem. B* **2008**, *112*, 1397.
(24) Zhang, X.; Borda, M. J.; Schoonen, M. A. A.; Strongin, D. R. *Langmuir* **2003**, *19*, 8787.
(25) Lin, K.-C.; Weis, R. M.; McConnell, H. M. *Nature* **1982**, *296*, 164.
(26) *Hazard Review: Health effects of occupational exposure to respirable crystalline silica*; NIOSH: Cincinnati, OH, **2002**; Vol. Publication No. *2002-129*.
(27) Fubini, B.; Fenoglio, I. *Elements* **2007**, *3*, 407.
(28) Murashov, V. V.; Harper, M.; Demchuk, E. *J. Occup. Environ. Hyg.* **2006**, *3*, 718.
(29) Nash, T.; Allison, A. C.; Harington, J. S. *Nature* **1966**, *210*, 259.
(30) Creuwels, L. A. J. M.; van Golde, L. M. G.; Haagsman, H. P. *Lung* **1997**, *175*, 1.
(31) Doughty, H. W. *J. Am. Chem. Soc.* **1924**, *46*, 2707.
(32) Stevens, M. J.; Donato, L. J.; Lower, S. K.; Sahai, N. *Langmuir* **2009**, *25*, 6270.
(33) Ma, G.; Allen, H. C. *Langmuir* **2006**, *22*, 5341.
(34) Gaines, G. L. *Insoluble monolayers at liquid-gas interfaces*; Interscience: New York, 1966.
(35) Chen, X.; Allen, H. C. *J. Phys. Chem. A* **2009**, *113*, 12655.
(36) Tang, C. Y.; Allen, H. C. *J. Phys. Chem. A* **2009**, *113*, 7383.
(37) *Handbook of optical constants of solids*; Palik, E. D., Ed.; Elsevier: New York, 1998.
(38) Zhuang, X.; Miranda, P. B.; Kim, D.; Shen, Y. R. *Phys. Rev. B* **1999**, *59*, 12632.
(39) Allen, H. C.; Casillas-Ituarte, N. N.; Sierra-Hernández, M. R.; Chen, X.; Tang, C. Y. *Phys. Chem. Chem. Phys.* **2009**, *11*, 5538.
(40) Casillas-Ituarte, N. N.; Allen, H. C. *Chem. Phys. Lett.* **2009**, *483*, 84.
(41) Chen, Z.; Shen, Y. R.; Somorjai, G. A. *Annu. Rev. Phys. Chem.* **2002**, *53*, 437.
(42) Du, Q.; Freysz, E.; Shen, Y. R. *Phys. Rev. Lett.* **1994**, *72*, 238.
(43) Richmond, G. L. *Chem. Rev.* **2002**, *102*, 2693.
(44) Shultz, M. J.; Schnitzer, C.; Simonelli, D.; Baldelli, S. *Int. Rev. Phys. Chem.* **2000**, *19*, 123.
(45) Stokes, G. Y.; Chen, E. H.; Buchbinder, A. M.; Walter, F. P.; Keeley, A.; Geiger, F. M. *J. Am. Chem. Soc.* **2009**, *131*, 13733.
(46) Roke, S.; Schins, J.; Müller, M.; Bonn, M. *Phys. Rev. Lett.* **2003**, *90*, 128101(1).

(47) Watry, M. R.; Tarbuck, T. L.; Richmond, G. L. *J. Phys. Chem. B* **2003**, *107*, 512.
(48) Shen, Y. R. *The principles of nonlinear optics*; John Wiley and Sons: New York, 1984.
(49) Aroti, A.; Leontidis, E.; Maltseva, E.; Brezesinski, G. *J. Phys. Chem. B* **2004**, *108*, 15238.
(50) Leontidis, E.; Aroti, A.; Belloni, L. *J. Phys. Chem. B* **2009**, *113*, 1447.
(51) Marcus, Y. *J. Chem. Soc., Faraday Trans.* **1991**, *87*, 2995.
(52) Volkov, V. V.; Takaoka, Y.; Righini, R. *J. Phys. Chem. B* **2009**, *113*, 4119.
(53) Jacobs, R. E.; White, S. H. *Biochemistry* **1989**, *28*, 3421.
(54) *Biological membranes: a molecular perspective from computation and experiment*; Merz, K. M. J., Roux, B., Eds.; Birkhauser: Boston, MA, 1996.
(55) Zhou, Z.; Sayer, B. G.; Hughes, D. W.; Stark, R. E.; Epand, R. M. *Biophys. J.* **1999**, *76*, 387.
(56) Yin, J.; Zhao, Y.-P. *J. Colloid Interface Sci.* **2009**, *329*, 410.
(57) Zhao, W.; Moilanen, D. E.; Fenn, E. E.; Fayer, M. D. *J. Am. Chem. Soc.* **2008**, *130*, 13927.
(58) Casal, H. L.; Mantsch, H. H.; Paltauf, F.; Hauser, H. *Biochim. Biophys. Acta* **1987**, *919*, 275.
(59) Hübner, W.; Mantsch, H. H. *Biophys. J.* **1991**, *59*, 1261.
(60) Arrondo, J. L. R.; Goñi, F. M.; Macarulla, J. M. *Biochim. Biophys. Acta* **1984**, *794*, 165.
(61) Binder, H.; Anikin, A.; Kohlstrunk, B.; Klose, G. *J. Phys. Chem. B* **1997**, *101*, 6618.
(62) Gauger, D. R.; Selle, C.; Fritzsche, H.; Pohle, W. *J. Mol. Struct.* **2001**, *565/566*, 25.
(63) Pohle, W.; Selle, C.; Fritzsche, H.; Bohl, M. *J. Mol. Struct.* **1997**, *408/409*, 273.
(64) Mrázková, E.; Hobza, P.; Bohl, M.; Gauger, D. R.; Pohle, W. *J. Phys. Chem. B* **2005**, *109*, 15126.
(65) Nagle, J. F.; Tristram-Nagle, S. *Biochim. Biophys. Acta* **2000**, *1469*, 159.
(66) Essmann, U.; Berkowitz, M. *Biophys. J.* **1999**, *76*, 2081.
(67) Satoh, K. *Biochim. Biophys. Acta* **1995**, *1239*, 239.
(68) Tatulian, S. A. *Eur. J. Biochemistry* **1987**, *170*, 413.
(69) Petrov, A. S.; Funseth-Smotzer, J.; Pack, G. R. *Int. J. Quantum Chem.* **2005**, *102*, 645.
(70) Potoff, J. J.; Issa, Z.; Manke, C. W., Jr.; Jena, B. P. *Cell. Biol. Int.* **2008**, *32*, 361.
(71) Marra, J.; Israelachvili, *J. Biochemistry* **1985**, *24*, 4608.
(72) Schneider, B.; Kabelác, M.; Hobza, P. *J. Am. Chem. Soc.* **1996**, *118*, 12207.
(73) Brumm, T.; Naumann, C.; Sackmann, E.; Rennie, A. R.; Thomas, R. K.; Kanellas, D.; Penfold, J.; Bayerl, T. M. *Eur. Biophys. J.* **1994**, *23*, 289.
(74) Dominguez, H.; Smondyrev, A. M.; Berkowitz, M. L. *J. Phys. Chem. B* **1999**, *103*, 9582.
(75) Högberg, C.-J.; Lyubartsev, A. P. *Biophys. J.* **2008**, *94*, 525.
(76) Smondyrev, A. M.; Berkowitz, M. L. *J. Comput. Chem.* **1999**, *20*, 531.
(77) Vácha, R.; Siu, S. W. I.; Petrov, M.; Böckmann, R. A.; Barucha-Kraszewska, J.; Jurkiewicz, P.; Hof, M.; Berkowitz, M. L.; Jungwirth, P. *J. Phys. Chem. A* **2009**, *113*, 7235.
(78) Griffin, R. G.; Powers, L.; Pershan, P. S. *Biochemistry* **1978**, *17*, 2718.
(79) Wang, H.-F.; Gan, W.; Lu, R.; Rao, Y.; Wu, B.-H. *Int. Rev. Phys. Chem.* **2005**, *24*, 191.
(80) Oh-e, M.; Yokoyama, H.; Baldelli, S. *Appl. Phys. Lett.* **2004**, *84*, 4965.
(81) Guan, Y.; Wurrey, C. j.; Thomas, G. J. *Biophys. J.* **1994**, *66*, 225.
(82) Tu, K.; Tobias, D. J.; Blasie, J. K.; Klein, M. L. *Biophys. J.* **1996**, *70*, 595.
(83) *Colloidal silica: Fundamentals and applications*; Bergna, H. E., Roberts, W. O., Eds.; CRC Taylor & Francis: Boca Raton, FL, 2006; Vol. 131, p 267.
(84) Iler, R. K. *The chemistry of silica: solubility, polimerization, colloid and surface properties, and biochemistry*; John Wiley and Sons. Willey-Interscience Publication: New York, 1979.
(85) Bickmore, B.; Tadanier, C. J.; Rosso, K. M.; Monn, W. D.; Eggett, D. L. *Geochim. Cosmochim. Acta.* **2004**, *68*, 2025.
(86) Sahai, N.; Sverjensky, D. A. *Geochim. Cosmochim. Acta* **1997**, *61*, 2801.
(87) Duval, Y.; Mielczarski, J. A.; Pokrovsky, O. S.; Mielczarski, E.; Ehrhardt, J. J. *J. Phys. Chem. B* **2002**, *106*, 2937.
(88) Chunbo, Y.; Daqing, Z.; Aizhuo, L.; Jiazuan, N. *J. Colloid Interface Sci.* **1995**, *172*, 536.
(89) Johnson, S. J.; Bayerl, T. M.; McDermott, D. C.; Adam, G. W.; Rennie, A. R.; Thomas, R. K.; Sackmann, E. *Biophys. J.* **1991**, *59*, 289.
(90) Tamm, L. K.; McConnell, H. M. *Biophys. J.* **1985**, *47*, 105.
(91) Castellana, E. T.; Cremer, P. S. *Surf. Sci. Rep.* **2006**, *61*, 429.
(92) Li, I.; Bandara, J.; Shultz, M. J. *Langmuir* **2004**, *20*, 10474.
(93) Ostroverkhov, V.; Waychunas, G. A.; Shen, Y. R. *Chem. Phys. Lett.* **2004**, *386*, 144.
(94) Naumann, C.; Brumm, T.; Bayerl, T. M. *Biophys. J.* **1992**, *63*, 1314.
(95) Roark, M.; Feller, S. E. *Langmuir* **2008**, *24*, 12469.
(96) Oleson, T. A.; Sahai, N. *Langmuir* **2008**, *24*, 4865.
(97) Xu, J.; Stevens, M. J.; Oleson, T. A.; Last, J. A.; Sahai, N. *J. Phys. Chem. C* **2009**, *113*, 2187.
(98) Murray, D. K.; Harrrison, J. C.; Wallace, W. E. *J. Colloid Interface Sci.* **2005**, *288*, 166.
(99) Sahai, N.; Sverjensky, D. A. *Geochim. Cosmochim. Acta* **1997**, *61*, 2827.
(100) Dove, P. M.; Craven, C. M. *Geochim. Cosmochim. Acta* **2005**, *69*, 4963.
(101) Jena, K. C.; Hore, D. K. *J. Phys. Chem. C* **2009**, *113*, 15364.
(102) Yang, Z.; Li, Q.; Chou, K. C. *J. Phys. Chem. C* **2009**, *113*, 8201.
(103) Karlsson, M.; Craven, C.; Dove, P. M.; Casey, W. H. *Aquat. Geochem.* **2001**, *7*, 13.
(104) Liu, J.; Conboy, J. C. *Langmuir* **2005**, *21*, 9091.
(105) Murashov, V. V.; Leszczynski, J. *J. Phys. Chem. A* **1999**, *103*, 1228.
(106) Hetzer, M.; Heinz, S.; Grage, S.; Bayerl, T. M. *Langmuir* **1998**, *14*, 982.

JP1022357